First physics results from the MAST Mega-Amp Spherical Tokamak

A. Sykes, J.-W. Ahn, R. Akers, E. Arends, P. G. Carolan et al.

Citation: Phys. Plasmas **8**, 2101 (2001); doi: 10.1063/1.1352595
View online: http://dx.doi.org/10.1063/1.1352595
View Table of Contents: http://pop.aip.org/resource/1/PHPAEN/v8/i5
Published by the American Institute of Physics.

First physics results from the MAST Mega-Amp Spherical Tokamak*

A. Sykes,[†,a)] J.-W. Ahn,[b)] R. Akers, E. Arends,[c)] P. G. Carolan, G. F. Counsell, S. J. Fielding, M. Gryaznevich, R. Martin, M. Price, C. Roach, V. Shevchenko, M. Tournianski, M. Valovic, M. J. Walsh,[d)] H. R. Wilson, and the MAST team
EURATOM/UKAEA Fusion Association, Culham Science Centre, Abingdon, Oxfordshire OX14 3DB, United Kingdom

(Received 24 October 2000; accepted 8 January 2001)

First physics results are presented from MAST (Mega-Amp Spherical Tokamak), one of the new generation of purpose built spherical tokamaks (STs) now commencing operation. Some of these results demonstrate, for the first time, the novel effects of low aspect ratio, for example, the enhancement of resistivity due to neo-classical effects. H-mode is achieved and the transition to H-mode is accompanied by a tenfold steepening of the edge density gradient which may enable the successful application of electron Bernstein wave heating in STs. Studies of halo currents show that these less than expected from conventional tokamak results, and measurements of divertor power loading confirm that most of the power flows to the outer strike points, easing the power handling on the inner points (a critical issue for STs). © *2001 American Institute of Physics.*
[DOI: 10.1063/1.1352595]

I. INTRODUCTION

The MAST (Mega-Amp Spherical Tokamak) device is designed to test the promising results obtained from the pioneering START (Small Tight Aspect Ratio Tokamak) experiment[1] operational at Culham from 1991 to 1998. MAST provides a test of the spherical tokamak (ST) concept in a large modern tokamak.

Operational results from the first MAST campaign, January–June 2000, were recently reported.[2,3] Both merging-compression and the more conventional solenoid induction start-up schemes have been demonstrated, the former providing an initial plasma current of over 400 kA with no solenoid flux. Good vacuum and operational conditions, particularly after boronization with trimethyl boron, have enabled the attainment of plasma current of over 1 MA with central electron and ion plasma temperatures of order 1 keV. The Hugill and Greenwald limits can be significantly exceeded, and H-mode achieved at modest additional neutral beam injection (NBI) power.

Here we present the initial physics results from this campaign, illustrating the insight that can be gained from studies of tokamak physics in the extreme of low aspect ratio.

II. NEO-CLASSICAL RESISTIVITY IN MAST

The tight aspect ratio of STs results in a large trapped particle fraction, so that neo-classical effects are enhanced relative to conventional tokamaks. STs therefore offer an ideal opportunity to test neo-classical theory. In MAST discharge #2735 Thomson scattering measurement of the electron density and temperature profiles indicates that the core plasma is in the banana collisionality regime. The magnetic equilibrium in this shot has been reconstructed using the SCENE code,[4] which solves the Grad–Shafranov equation using density and temperature profiles provided by 30-point Thomson scattering. It is assumed that the central temperature of the ions is as indicated by the neutral particle analyzer (NPA) diagnostic and they have the same radial profile as electrons; impurity contributions and the effect of collisionality, which reduce the trapped fraction, are included. The current profile can be specified to be that predicted by neo-classical theory, from which SCENE provides an estimate of the loop voltage (assumed to be constant across the plasma). This reconstruction is shown in Fig. 1, together with an optical image of the MAST plasma.

The sawtooth inversion radius in #2735, measured from the soft x-ray data, is 30 ± 5 cm in the vertical direction, and is constant over four sawtooth periods, suggesting that the current profile is no longer evolving (and therefore that the loop voltage is indeed approximately constant outside the $q=1$ surface).

The position of the $q=1$ surface determined by SCENE is shown in Fig. 1, and is close to the observed sawtooth inversion radius. This is an indication that the current profile outside $q=1$ is consistent with that expected from neo-classical theory. The collisionality ν_e^* is ~ 0.15 within the $q=1$ surface shown in Fig. 1, rising to ~ 0.5 at the $q=2$ surface.

The loop voltage measured in #2735 is 1.5 V, which is matched by the SCENE neo-classical calculation assuming a plausible $Z_{\text{eff}}=1.8$. If we perform the same calculation assuming Spitzer conductivity we find that the loop voltage is 0.6 V, too low to explain the data for any reasonable Z_{eff}. The neo-classical current profile is very peaked, and SCENE, in the absence of any sawtooth model, predicts $q_0 \sim 0.35$ (the

*Paper GI1 2, Bull. Am. Phys. Soc. **45**, 117 (2000).
†Invited speaker.
a)Electronic mail: alan.sykes@ukaea.org.uk
b)Also at Imperial College of Science, Technology and Medicine, University of London, London SW7 2BZ, UK.
c)Also at FOM Insituut voor Plasmafysica 'Rijnhuizen,' Postbus 1207, 3430 BE Nieuwegein, The Netherlands.
d)Also at Walsh Scientific Ltd., Abingdon, Oxon OX14 3DB, UK.

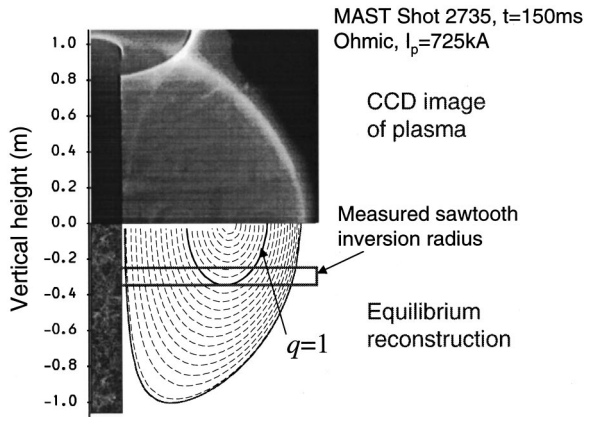

FIG. 1. Modeling of Ohmic MAST #2735 (CCD image shown above) by SCENE.

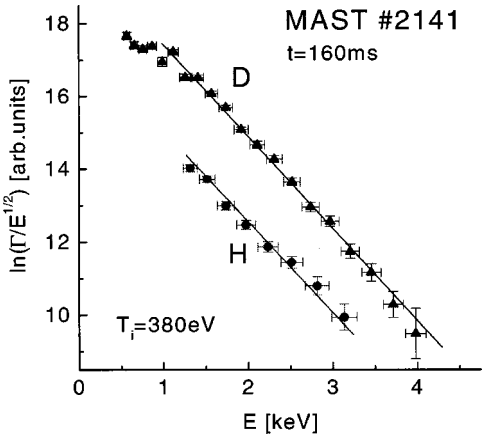

FIG. 2. NPA energy spectra for both H and D in Ohmic MAST #2141.

Spitzer model predicts $q_0 \sim 0.7$). We would therefore expect that the sawtooth activity present in the experiment would re-distribute the current over the central region of the plasma. Although this would have only a small effect for the example studied here it could be significant for higher current scenarios where the $q=1$ surface is at larger radius.

While these are very preliminary results, and considerably more data and analysis are needed, the evidence presented is self-consistent and supports the assumption that neo-classical effects do play a dominant role in ST physics. One consequence of these neo-classical effects would be that ST plasmas have an enhanced power input compared to an equivalent conventional tokamak of the same current, because $V_{\text{loop}} > 2 \times V_{\text{Spitzer}}$. This may account for the relative ease with which even Ohmic MAST plasmas can exceed the Greenwald density limit.[3] This effect should be even greater in higher performance MAST plasmas with higher temperatures and hence lower collisionality, for which similar modeling predicts $V_{\text{loop}} \sim 4 \times V_{\text{Spitzer}}$.

III. NEUTRAL BEAM HEATING ON MAST

MAST is equipped with two neutral beam injection (NBI) lines on loan from the Oak Ridge National Laboratory. At full specification, they are together designed to deliver 5 MW of deuterium neutrals at energies up to 30 keV. During the first campaign, the South injector alone was operational, delivering up to 800 kW of hydrogen neutrals at energies up to 35 keV. An $E \| B$ neutral particle analyzer (NPA), on loan from the Princeton Plasma Physics Laboratory, has been installed at a tangency radius of 0.7 m to diagnose the fast ion population resulting from NBI injection, and measure changes in the bulk thermal plasma temperature. The NPA can measure particle energies from 0.5 to 600 keV/amu for hydrogen and deuterium simultaneously. It is found that Ohmic plasmas generally yield an energy spectrum characterized by a single temperature as shown in Fig. 2. However, after strong magneto-hydrodynamic (MHD) activity, such as an Internal Reconnection Event (IRE) or even sustained sawtooth activity, a pronounced high-energy tail can be produced.[5,6] A tail extending above the beam injection energy is also routinely observed during NBI.

Although the NBI power and energy used to date is very similar to that employed on START, beam heating (and current drive) are predicted to be more effective on MAST due to the higher fields and temperatures and larger plasma size. Electron and ion temperatures measured for a large range of discharge conditions are shown in Fig. 3; START data[7] are also shown. The lines shown in Fig. 3 are predictions of a simple thermal ion power balance. The lower curve is for Ohmic plasmas, assuming a lower bound for energy confinement based on first experimental estimates (see Sec. V). The upper curve assumes the maximum value of the power, P_i^{NBI}, absorbed by the ions for this first campaign (derived from the LOCUST Monte Carlo code), together with an upper estimate of the energy confinement time.

IV. ENERGY CONFINEMENT

START ELMY (i.e., with edge localized modes) H-mode confinement data have previously been represented by ITER98PBY1 scaling,[3,8] and are slightly below the predic-

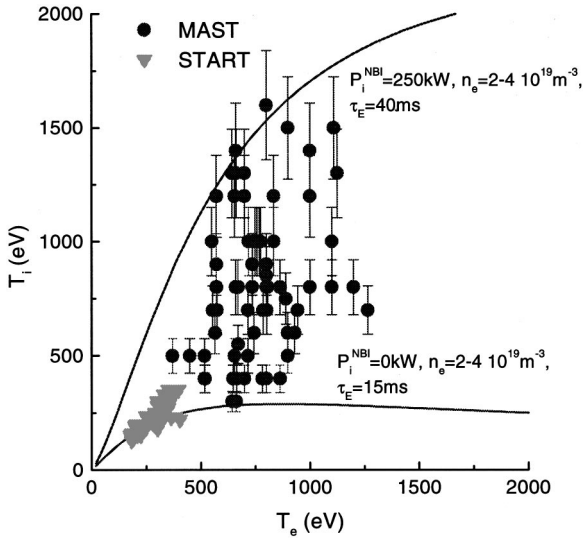

FIG. 3. Plot of central T_e (from Thomson scattering) and T_i temperatures (deduced from NPA measurements) for NBI heated discharges during the first campaign. The curved lines indicate the maximum and minimum predictions of simple thermal power balance modeling.

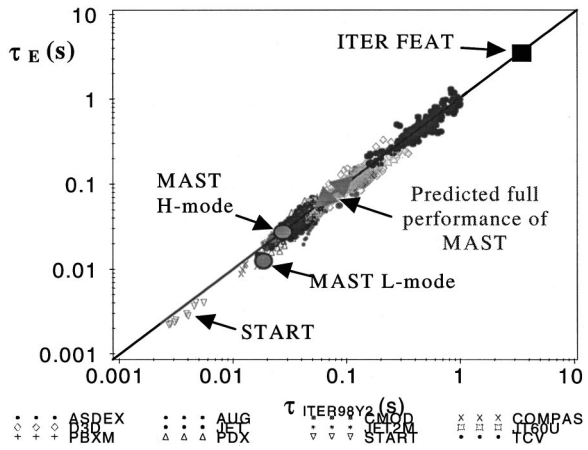

FIG. 4. World tokamak ELMy H-mode confinement data, compared with the ITER98PBY2 scaling. Data from International Confinement Database DB03V5 [IPB] with new COMPASS and START data as submitted to DB03V9, and preliminary MAST data.

tions of the ITERPBY2 variant now generally adopted, as shown in Fig. 4. We shall now use the PBY2 form in order to compare directly with conventional tokamaks. A notable feature of H-mode discharges on START was that a clear improvement in confinement (compared to similar L-mode discharges) was only found at the highest plasma currents (>250 kA) achievable.[8] Modeling suggests[9] that this is due to the very high neutral density present in START, which caused increased charge–exchange losses at transition. In MAST, however, the neutral density in the vacuum tank is typically 50 times lower for the same plasma density, as shown in Fig. 5. The same wall conditioning techniques

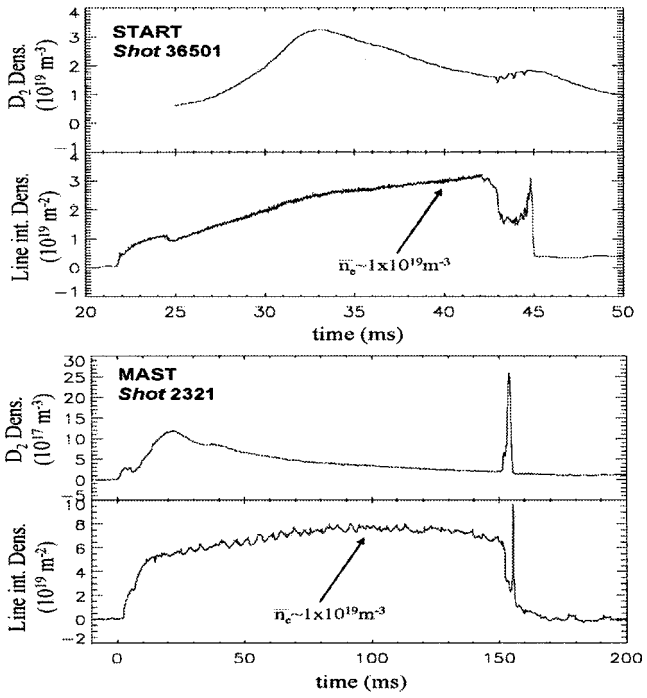

FIG. 5. Waveforms of vacuum neutral gas pressure, measured by a fast ion gauge at the vessel wall, and line integral plasma density. In this example the neutral pressure in START was 40 times higher than in MAST for the same line-average plasma density of 1×10^{19} m^{-3}.

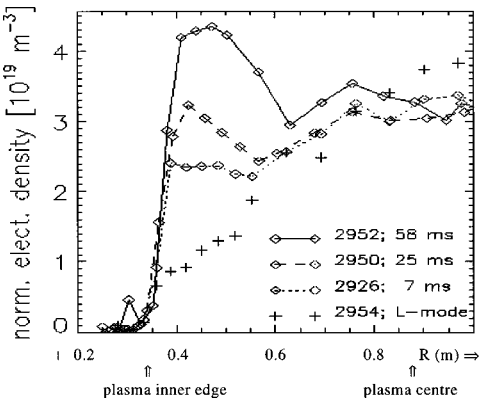

FIG. 6. Development of density profile at the inboard edge, during initial ELM-free period after first L-H transition.

(glow discharge cleaning, boronization with tri-methylated boron) and the same plasma contact surfaces (graphite) were used in both devices, and the difference in neutral density is mainly due to the increased particle confinement time in the larger device. In addition, the high gas puff used during the merging-compression plasma formation[3] remained during the short pulse of START but is a transient in the much longer duration MAST discharges.

H-mode operation has been established in MAST.[2,3] First analysis[3] shows that in contrast to START, H-mode discharges on MAST exhibit a clear increase in confinement even at low currents, attaining $H_{\mathrm{PBY2}}\sim1$. This first MAST data are shown in Fig. 4; the energy confinement in L-mode was ~14 ms, increasing to 28 ms in H-mode.

If the ITERPBY2 scaling continues to apply to MAST at full design performance (2 MA, density at 0.7×Greenwald), this would predict confinement times in the range 55 ms (with 6 MW of additional heating) to 120 ms (Ohmic), as indicated in Fig. 4.

V. FEATURES OF H-MODE IN MAST

The electron density profile exhibits remarkable features on first transition to ELM-free H-mode, as seen on the Thomson scattering profiles shown in Fig. 6. In this figure profiles from several similar shots are overlaid; the densities are normalized to the average line-average density before transition, and the times indicate the time elapsed since the start of the ELM-free period. A discharge with similar parameters, but which did not undergo L-H transition, is shown for comparison. The development of ''ears'' after transition is clearly seen. The ear is mainly a result of changes in transport, as modeling indicates that fueling from the 30 keV NBI can account for only approximately 25% of the increased density. Subsequent ELMs act to degrade the ''ear'' but the general form is retained, in particular the steep edge gradient. No clear changes in the electron temperature profile are observed during the development of the steep density profiles.

In #2952 the line-average density increases from ~2.3 $\times10^{19}$ m^{-3} to ~3.3$\times10^{19}$ m^{-3} during the 58 ms ELM-free period before the Thomson scattering profile was obtained. The profiles shown in Fig. 6 indicate that the increase

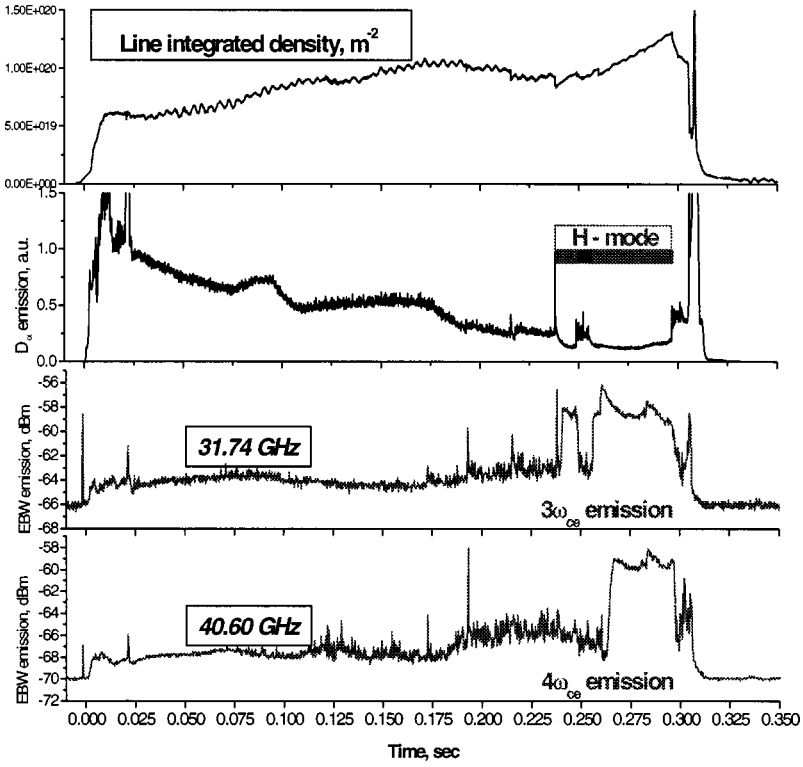

FIG. 7. Line integrated density midplane D_α signal and 31.74, 40.60 GHz EBW radiometer signals during L-H transition in NBI heated MAST #2942.

in line-average density observed after L-H transition is principally due to increased density at the edge of the plasma. The development of this steep edge gradient opens up a promising new application, discussed in the next section.

VI. EBW EMISSION IN MAST

It has been suggested[10] that electron Bernstein wave (EBW) could be a valuable tool for heating and current drive in STs, as Bernstein waves have no high density cutoff and can penetrate toward the center of the plasma with $\omega_{pe} \gg \omega$. It is proposed to investigate EBW heating on MAST via the existing 60 GHz ECRH facility; as a first step an EBW radiometer has been installed on MAST designed to study the EBW emission, which may escape the plasma via the Bernstein–extraordinary–ordinary (B-X-O) mode conversion mechanism. Radiometer signals from high density plasmas are usually very low, and the frequencies observed are well below the central plasma frequency. This is because, although the B-X-O conversion efficiency can be high (close to 100%), this is only for a narrow angular cone around the optimal direction. For example, in MAST plasmas with $n_{e0} = 1.5\times10^{20}$ m^{-3} and a parabolic density profile the conditions of efficient mode conversion define the elliptical angular cone with $\delta\theta_y = \pm 3.7°$ (angle in the plane spanning the density gradient and magnetic field) and $\delta\theta_z = \pm 5.6°$ (angle in the perpendicular plane) for the 60 GHz electron cyclotron resonance heating (ECRH) to be used in MAST.[11] It is quite difficult to match these conditions in practice. Even for a particular plasma scenario the optimum angle is changed significantly during the shot because of changes in plasma size and current.

The situation is totally different in H-mode plasmas. The B-X-O conversion efficiency is exponentially dependent on the density gradient, especially on the gradient at the O-mode cutoff layer, where the X-O mode conversion occurs. So with steeper edge density gradients one can expect high mode conversion efficiency in a wider range of angles. As shown in Fig. 6, following the L-H transition in MAST the edge density gradients grow from $\sim10^{20}$ m^{-4} up to $\sim10^{21}$ m^{-4} in the density range of $(0.5–4)\times10^{19}$ m^{-3}. The angular window for efficient conversion is then increased by more than a factor of 3.

This effect has been observed experimentally during the H-mode campaign on MAST, which featured NBI heating but no applied ECRH. Figure 7 illustrates the behavior of EBW signals presented on a logarithmic scale during H-mode shot #2942. Before the L-H transition the EBW signal at 31.74 GHz (corresponding to the third harmonic at the outer edge) has a relatively low level, about -66 dB m with short spikes coincident with sawteeth. Plasma density is high enough to prevent direct emission from electron cyclotron harmonics because in this shot all harmonics up to the fifth are trapped by cutoffs in the bulk plasma. So this emission can be explained by B-X-O mode conversion with low conversion efficiency due to the mismatch of the receiving angular cone and the receiving cone centered around the viewing angle chosen to be 28° to the midplane and 20° to the major radius, at a distance of 20 cm below the midplane. In this discharge there is a short H-mode period at 238 ms, with emission observed from the second and third harmonics, the EBW signal instantly increasing by 8 dB. A longer ELM-free period is established at a time of 255 ms and the increased edge density gradient leads to a strong emission at 40.60 GHz, from the $4\omega_{ce}$ resonance. This emission is sustained until the H-mode starts to degrade, following the re-

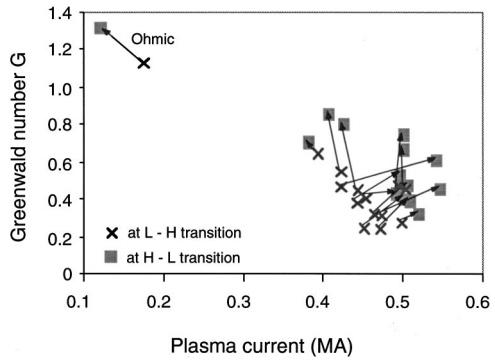

FIG. 8. H-mode operation space (January–June 2000) showing location of L-H transition and final H-L back transition in normalized density G $(=n/n_G)$ and plasma current space. All NBI initiated, DND H-mode discharges are shown, together with Ohmic, limited discharge #2910.

moval of the Ohmic drive (V_{loop} is set to zero) from $t\sim 275$ ms.

These results from MAST are the first observation of EBW emission at third and fourth harmonics and suggest that the narrow angular window required for high conversion efficiency becomes much wider for the extreme density profiles associated with the H-mode in MAST. This suggests that EBW heating could indeed be feasible in STs, and it is proposed to investigate this via the existing 60 GHz ECRH facility. Assuming the same behavior of the edge density profile during H-mode at higher central densities ($>4.5\times 10^{19}$ m^{-3}), one can estimate the angular window for 60 GHz to be as large as $\delta\theta_y=\pm 37°$ and $\delta\theta_z=\pm 56°$, although the WKB approximation becomes questionable when the density scale length is less than the wavelength.

VII. H-MODE AT HIGH DENSITY

In this first campaign on MAST, L-H transition for large, double-null diverted (DND), NBI heated plasmas occurred at Greenwald numbers $G=0.2$ to 0.65, where $G=n/n_G$ and n_G is the Greenwald density, $=I/(\pi a^2)$. The loci of the H-mode phase of all these discharges are shown in Fig. 8. Note that in all cases, G increases after the L-H transition. The highest normalized density achieved while in H-mode was $G\sim 0.85$ in #2926. Attempts during this campaign to raise further the density produced peaked discharges with frequent central sawteeth; if the heavy gas puffing was removed, the sawtooth period lengthened, the $q=1$ radius broadened, and L-H transition could then take place, however at $G<1$.

In addition to these large, DND NBI-initiated H-mode plasmas, high density Ohmic operation often produced L-H transition during the plasma current decay stage, when the plasmas were limited on the center column. These plasmas are relatively small (typical minor radius 25–28 cm, major radius 45–48 cm), with low elongation ($k\sim 1.2$–1.3), but may still be regarded as of low aspect ratio since $A\leqslant 1.8$. In shot #2910 L-H transition happens after a MARFE appears at $n/n_G\sim 1.3$. This shot is also indicated in Fig. 8. The plasma current decreases because of the negative loop voltage applied at the end of the shot.

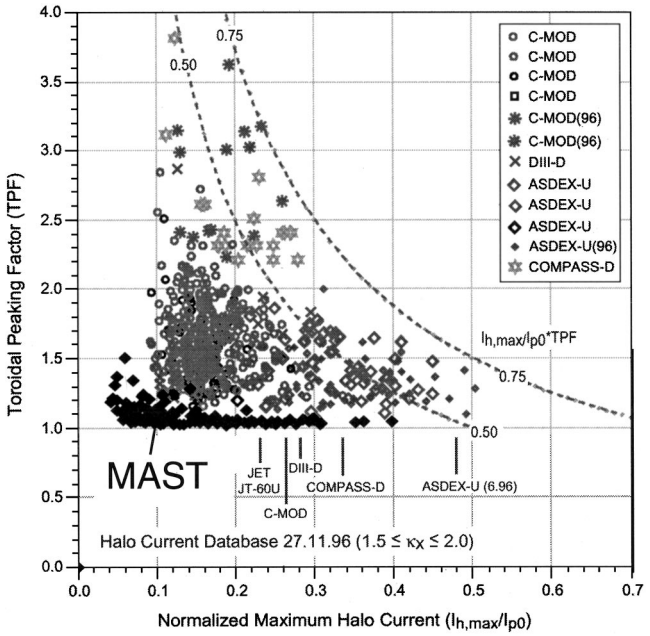

FIG. 9. Halo current fraction, and toroidal peaking factor (TPF), calculated at time of maximum halo current. All MAST low-aspect-ratio data are shown.

VIII. HALO CURRENT STUDIES IN MAST

Although theory and modeling predict that forces due to halo currents should be relatively low in the ST,[12,13] it is important to verify this as MAST is designed for operation up to 2 MA, and so a comprehensive set of halo current diagnostics have been installed and commissioned.[14] Results at low aspect ratio should also serve as a test of the theories of halo currents.

Results are shown in Fig. 9. In this plot all MAST vertical displacement event (VDE) data for low aspect ratio plasmas ($A<1.8$) are shown. It is seen that the toroidal peaking factor (TPF) is very low—that is, the halo currents produced are very symmetric. This is consistent with the observation[13] that at low aspect ratio, the toroidal eddy current paths around the center column have a similar impedance to the poloidal paths. Hence the currents induced at a VDE become very symmetric, leading to much lower forces than those met in tokamaks of conventional aspect ratio.

The line $I_{\text{halo}}/I_{\text{plasma}}\times\text{TPF}=0.5$ indicated in the diagram is a typical design constraint for the International Thermonuclear Experimental Reactor–Fusion Energy Advanced Tokamak ITER-FEAT.[15]

IX. DIVERTOR POWER LOADING STUDIES

MAST is well equipped with arrays of high spatial resolution, swept Langmuir probe arrays (576 probes in total) covering all four strike point regions[16] (Fig. 10). For Ohmic plasmas, densities and temperatures in both the outboard and inboard scrape-off-layers (SOLs) produce strongly collisional conditions ($\nu_e^*>7$ and 50, respectively) with midplane heat flux density scale lengths of order 6 mm at both

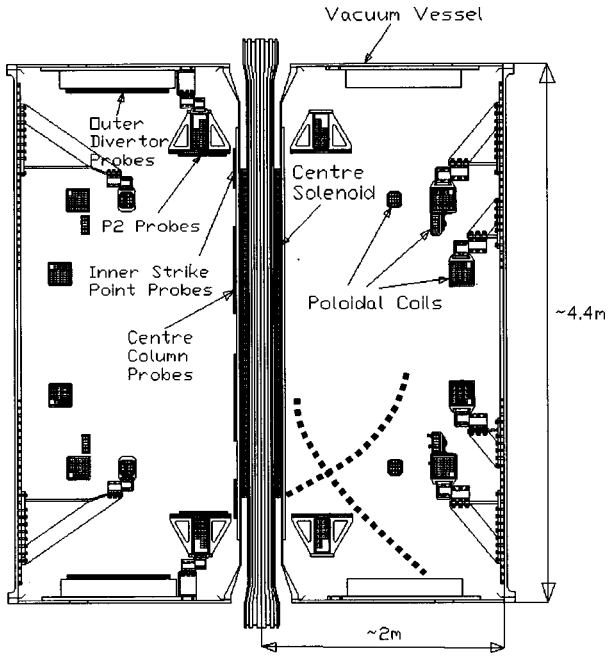

FIG. 10. Location of Langmuir probes (576 in all) in MAST. Strike point locations (see Fig. 11) are indicated for a typical DND plasma.

positions. All the plasma parameter scale lengths are significantly increased on the outboard side as a result of strong poloidal flux expansion (Fig. 11).

About two-thirds of the power entering the SOL reached the targets,[16] compared to one third on START (the difference probably arising from higher charge exchange losses in START). The ratio of the power to the outboard targets to the power to the inboard targets was 9:1 in L-mode discharge 2951, shown in Fig. 11. Hence the power loading on the inboard strike point may not be as critical for the ST as was initially supposed. In this discharge the peak divertor load occurred at the inboard strike point, and was 0.72 MW/m^2 for a total input power of ~1.5 MW; at full design performance of MAST (approx. 2 MW Ohmic input, 6 MW auxiliary heating) this would correspond to a tolerable peak load of ~3.8 MW/m^2. However, heat flux density scale lengths could be reduced, and inboard/outboard ratios different, in H-mode conditions; this will be investigated in the next campaign.

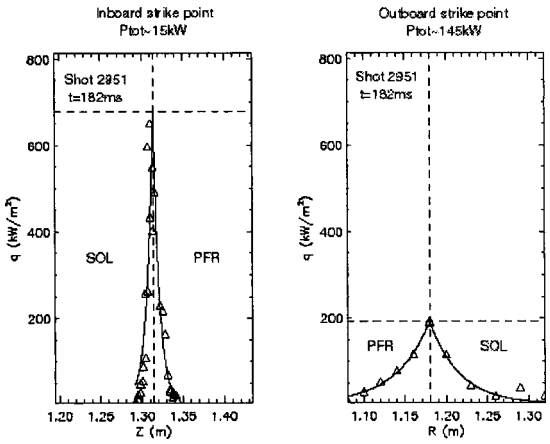

FIG. 11. Heat flux density profiles across the inboard and outboard strike points in L-mode shot 2951. The total input power to the plasma is ~1.49 MW (approx. 0.72 MW Ohmic, 0.77 MW NBI). The peak divertor load is ~0.7 MW/m^2 on the inboard.

X. CONCLUSIONS

The first six months of MAST operations have been remarkably successful, both operationally (as described in Refs. 2, 3) and in the physics results obtained. These results, together with those from the other new STs now commencing operation, will rapidly increase the understanding of the physics properties of the ST and determine its potential for a future fusion device.

ACKNOWLEDGMENTS

This work is funded jointly by the U.K. Department of Trade and Industry and EURATOM. The NBI equipment is on loan from the Oak Ridge National Laboratory, and the NPA from the Princeton Plasma Physics Laboratory.

[1] A. Sykes and the START, NBI, MAST and Theory Teams, Nucl. Fusion **39**, 1271 (1999).
[2] M. Gryaznevich and the MAST Team, ''First results from MAST,'' in Proceedings of the 27th European Conference on Controlled Fusion and Plasma Physics, Budapest, 2000 (European Physical Society, Petit-Lancy).
[3] A. Sykes, in Proceedings of 18th IAEA Fusion Energy Conference, Sorrento, 2000, Nucl. Fusion (to be published).
[4] H. R. Wilson, Nucl. Fusion **32**, 257 (1992).
[5] R. J. Akers, L. C. Appel, E. Arrends *et al.*, ''On the neutral beam heating of spherical tokamak plasmas,'' in Proceedings of 18th IAEA Fusion Energy Conference, Sorrento, 2000, Nucl. Fusion (to be published).
[6] M. R. Tournianski, R. J. Akers, C. A. Bunting, C. Byrom, P. G. Carolan, and N. J. Conway, Bull. Am. Phys. Soc. **45**, 341 (2000).
[7] P. G. Carolan, N. J. Conway, M. R. Tournianski *et al.*, *Proceedings of the 24th European Conference Controlled Fusion and Plasma Physics*, Berchtesgaden (European Physical Society, Geneva, 1997), Vol. 21A, P1 241.
[8] A. Sykes, R. Akers, L. Appel *et al.*, Phys. Rev. Lett. **84**, 495 (2000).
[9] Yu. Dnestrovskij, M. P. Gryaznevich, A. Yu. Dnestrovskij *et al.*, Plasma Phys. Rep. **26**, 539 (2000).
[10] R. A. Cairns and C. N. Lashmore-Davies, Phys. Plasmas **7**, 4126 (2000).
[11] V. F. Shevchenko, ''ECE measurements via B-X-O mode conversion—A proposal to diagnose the q profile in spherical tokamaks,'' Plasma Phys. Rep. (to be published).
[12] A. Caloutsis and C. G. Gimblett, Nucl. Fusion **38**, 1487 (1998).
[13] N. Pomphrey, J. M. Bialek, and W. Park, Nucl. Fusion **38**, 449 (1998).
[14] R. Martin, R. J. Buttery, G. C. Cunningham *et al.*, in Proceedings of the 27th European Conference on Controlled Fusion and Plasma Physics, Budapest, 2000 (European Physical Society, Petit-Lancy), P1.041.
[15] R. Yoshino, D. J. Campbell, E. Fredrickson *et al.*, in Proceedings of 17th IAEA Fusion Energy Conference, Yokohama (1998), ITERP1/14 (IAEA Sales & Promotion Unit, PO Box 100, Vienna).
[16] G. F. Counsell, J-W. Ahn, S. J. Fielding, and G. P. Maddison, in Proceedings of the 27th European Conference on Controlled Fusion and Plasma Physics, Budapest, 2000, P4.088 (European Physical Society, Petit-Lancy).